Disrupted structural connectivity in Pediatric Bipolar Disorder

Henrique M. Fernandes[1,2,3], Joana Cabral[1,3,4], Tim J. Van Hartevelt[1,3], Louis-David Lord[1], Carsten Gleesborg[2,5], Arne Moller[2], Gustavo Deco[6,7], Peter C. Whybrow[8], Predrag Petrovic[9], Anthony C. James [1,10], and Morten L. Kringelbach[1,2,3,4]

[1] *Department of Psychiatry, University of Oxford, Oxford, OX3 7JX, UK;*

[2] *Center of Functionally Integrative Neuroscience (CFIN), Aarhus University, Aarhus, Denmark;*

[3] *Center for Music in the Brain (MIB), Aarhus University, Aarhus, Denmark;*

[4] *Life and Health Sciences Research Institute (ICVS), School of Medicine, University of Minho, 4710-057 Braga, Portugal;*

[5] *Sino-Danish Center for Education and Research (SDC)*

[6] *Theoretical and Computational Neuroscience Group, Center of Brain and Cognition, Universitat Pompeu Fabra, Barcelona, 08018, Spain;*

[7] *Institució Catalana de Recerca i Estudis Avançats (ICREA), Barcelona, 08010, Spain;*

[8] *Semel Institute for Neuroscience and Human Behavior, University of California, Los Angeles, USA;*

[9] *Cognitive Neurophysiology Research Group, Department of Clinical Neuroscience, Karolinska Institute, Stockholm 171 76, Sweden;*

[10] *Highfield Unit, Warneford Hospital, Oxford, OX3 7JX, UK.*

Abstract

Background: Bipolar disorder (BD) has been linked to disrupted structural and functional connectivity between prefrontal networks and limbic brain regions. Studies of patients with pediatric bipolar disorder (PBD) can help elucidate the developmental origins of altered structural connectivity underlying BD and provide novel insights into the aetiology of BD.

Methods: The network properties of whole-brain structural connectomes, constructed using probabilistic tractography and diffusion tensor imaging (DTI), were compared between groups of un-medicated PBD patients with psychosis euthymic and matched healthy controls. Specific network measures were correlated with neurocognitive and psychotic scores, thus providing a comprehensive characterization of topological brain changes underlying PBD.

Results: Widespread changes in the structural connectivity of PBD patients were found in both cortical and subcortical networks, notably affecting the orbitofrontal cortex, frontal gyrus, amygdala, and hippocampus. Graph theoretical analysis revealed that PBD connectomes have fewer hubs, weaker rich club organization, different modular structure and increased network asymmetries compared to healthy participants. Moreover, patients' IQ and psychotic symptoms significantly correlated with the local efficiency of the orbitofrontal cortex.

Conclusion: The results show that PBD is associated with significant changes in structural network topology, which may indicate a reduced capacity for balanced whole-brain integration of information. Localized network changes involve brain regions associated with emotional processing and regulation, as well as cognitive processing, some of which correlate with cognitive and clinical measures. These findings suggest that structural brain connectivity changes may contribute to the deficits in emotion processing and regulation found in PBD.

Introduction

Bipolar disorder (BD) is a psychiatric illness characterized by episodes of mania or hypomania and depression interleaved with euthymic periods. It has been suggested that prefrontal control over emotional networks is deficient in BD, inducing abnormally heightened emotional and reward processing in patients (1–4).

Functional neuroimaging studies of euthymic bipolar patients have shown both reduced activity in the prefrontal cortex (PFC), especially in the ventrolateral and ventromedial PFC , and increased activity in emotional processing areas such as the ventral striatum (5), the amygdala (6) and the insula (7,8) whilst performing a range of emotional processing tasks, Similar activity patterns in PFC were also observed in manic (3) and depressed (9,10) episodes. Moreover, functional connectivity studies have suggested a decreased coupling between frontal and limbic areas (10), which might reflect abnormalities in the way these regions jointly process information in BD.

In contrast, structural neuroimaging studies are not dependent on the choice of an experimental task. The need for higher statistical power and convergence of the findings has motivated the production of several large voxel-based meta-analyses (11–13), as well as large single-centre studies (14). These structural studies have found decreased brain volume in BD in a specific set of brain regions including medial PFC, anterior cingulate cortex and ventrolateral PFC as well as the insula.

In addition to volumetric analyses, studies of structural connectivity in BD, which serves as the structural substrate over which the repertoire of functional networks can unfold, can provide highly valuable insights into the neural mechanisms underlying this disorder. Diffusion imaging studies have found altered structural connectivity between hemispheres (15), as well as prefrontal and subcortical regions in BD, which may result in abnormal communication between these regions and disrupt the modulation of emotional processing, onset of mania and the development of bipolar disorder (2,16–18).

In summary, there is emerging evidence linking BD to altered functional and structural connectivity between prefrontal regions and emotion processing regions such as the insula and the amygdala. BD most often starts in childhood or adolescence with sub-clinical or clinical manifestations of the disorder, suggesting an important developmental component (19). Pediatric bipolar disorder (PBD) is a cyclic mood disorder in children and adolescents, which can be persistent and severe, and has an estimated prevalence of around 1% (20). Although abnormal functional connectivity is proposed to be

a main feature in BD, few studies have focused on whether the underlying structural connectivity is altered in BD using state-of-the-art whole-brain network analysis (21–23). As such, studying patients with PBD would help to minimise potentially confounding secondary manifestations of BD and help clarify the neural mechanisms inducing and maintaining manic and depressed states in BD.

Here we constructed the structural connectomes of a group of adolescents with PBD and psychosis and of closely matched healthy controls. We used advanced structural connectomics analysis to characterise the topological differences in structural connectivity driving the cognitive and emotional symptoms found in PBD.

Methods

Participants

We analysed data from 15 patients with PBD with psychosis from the Oxford regional unit and surrounding units, and 15 euthymic age- and gender-matched healthy controls (HC) (Table 1). The patients were diagnosed according to the DSM-IV-TR criteria using the Kiddie Schedule for Affective Disorders and Schizophrenia (K-SADS-PL), and were administered the Positive and Negative Syndrome Scale (PANSS). The healthy subjects were recruited from the community through their general practitioners and interviewed using the K-SADS-PL to rule out any history of emotional, behavioural, or medical problems. Handedness was assessed with the Edinburgh Handedness Questionnaire. Intellectual ability was assessed using the Wechsler Abbreviated Scale of Intelligence (WASI). All subjects were clinically reviewed after the initial diagnostic screening for a period of at least six months (mean±std; 10±1.5 months); no subject changed diagnostic status. James and colleagues previously reported a comprehensive description of the cohort and clinical assessment strategy used in this study (2).

Image acquisition

All 30 participants underwent the acquisition of whole-brain T1-weighted and diffusion-weighted images using a 1.5 T Sonata magnetic resonance imager (Siemens, Erlangen, Germany) with a standard quadrature head coil and maximum 40 mT / m gradient capability. The 3D T1-weighted FLASH sequence was performed with the following parameters: coronal orientation; 256 x 256 reconstructed matrix; 208 slices; 1x1 mm^2 in-plane resolution; slice thickness of 1 mm; echo time (TE) of 5.6 ms; repetition time (TR) of 12 ms; flip-angle (α) of 19°. The diffusion-weighted sequences were obtained using echo-planar imaging (SE-EPI), and its scanning parameters were: TE of 89 ms; TR of 8500 ms; 60 axial slices; bandwidth = 1860 Hz/vx; voxel size of 2.5 x 2.5 x 2.5 mm^3); 60 isotropically distributed orientations for the diffusion-sensitising gradients at a b-value of 1000 s/mm^2 and five b0 images. To increase signal-to-noise ratio, scanning was repeated three times and all scans were merged.

Network construction

The construction of the brain structural network for each experimental group consisted of a two-step process. First, the nodes of the network were defined using a brain parcellation. Secondly, the

connections between nodes (i.e. edges) were estimated using probabilistic tractography. In the following we outline the details involved in each step.

Brain parcellation

For each subject, the brain was parcellated in native DTI space into 90 different cortical and subcortical regions using the Automated Anatomical labelling (AAL) template (24), where each region represents a node in the brain network.

Flirt (FMRIB, Oxford) (25) was used to linearly co-register the standard ICBM152 in MNI space (26) to each native T1-weighted structural image of each subject, using an affine registration (12 DOF) combined with a nearest-neighbour interpolation method. The resulting transformation was further applied to warp the Automated Anatomical Labeling (AAL). The MRI-DTI scan was then converted to MRI-T1 space, using a rigid-body transformation (6 DOF) and the resulting transformation matrix inverted. The MNI to MRI-T1 and MRI-T1 to MRI-DTI transformation matrices were subsequently concatenated, allowing a direct co-registration of the AAL template in MNI space to the diffusion MRI native space. This last transformation was performed using a nearest-neighbour interpolation method to ensure that discrete labelling values were preserved.

Brain structural network

We used the FDT toolbox in FSL (version 5.0, http://www.fmrib.ox.ac.uk/fsl/, FMRIB, Oxford) to carry out the multiple processing stages of the diffusion MRI data. The initial pre-processing involved correction of head motion and eddy current gradient induced image distortions. Subsequently, we modelled for crossing fibres within each voxel of the brain using a Markov Chain Monte Carlo sampling algorithm to build up distributions on diffusion parameters and estimate the local probability distribution of fibre direction at each voxel of the brain. (27) For this step, we used an automatic estimation of two fibre directions within each voxel, in order to improve the tracking sensitivity of non-dominant fibre populations in the human brain. (28)

Probability of connectivity was estimated using probabilistic tractography at the voxel level, with a sampling number of streamline fibres per voxel set at 5000. Brain boundaries were defined based on a binary brain previously registered in a skull-extracted version of the subject's native brain. The connectivity from a seed voxel i to another voxel j was defined by the proportion of streamlines leaving voxel i and reaching voxel j. (28) This was then extended from the voxel to the region level, i.e. in a brain region consisting of n voxels, $5000*n$ fibres were sampled. The connectivity probability

P_{ij} from region i to region j is then calculated as the number of sampled fibres in region i connecting the two regions, divided by 5000*n, where n is the number of voxels in region i. For each brain region, the connectivity probability to each of the remaining 89 AAL regions was calculated. The regional connectivity probability was computed using in-house Perl scripts and further normalised by each region's volume, expressed in number of voxels. It should be noted that, given the dependence of tractography on the seeding location, the probability from i to j is not necessarily the same to that from j to i. However, these two probabilities are highly correlated across the brain for all participants. We therefore defined the undirectional connectivity probability P_{ij} between regions i and j by averaging these two probabilities. We considered this as a measure of the structural connectivity between each pair of areas, with $C_{ij}=C_{ji}$.

For each participant, a 90x90 symmetric weighted matrix C was constructed, representing the brain's structural network.

Graph Theorethical Analysis

Standard Graph Metrics. The structural brain networks, represented as a 90x90 connectivity matrix, can be analysed as graphs. Using the Brain Connectivity Toolbox (29), the brain networks were characterized using measures from graph theory. A rescaled version of the structural networks, where individual networks are normalised by its maximum connectivity value, was used. The following standard local and global graph metrics were considered: Connection Density, Node Degree, Local Efficiency, Global Efficiency, Characteristic Path length, Clustering Coefficient and Small-World index. Definitions and equations for these measures can be found in Supplementary Information.

Modularity. Modularity quantifies the degree to which the network may be subdivided into non-overlapping communities. Therefore, the optimal community structure is represented as a subdivision of the network into well-defined groups of nodes so that it maximizes the number of within-group edges and minimizes the number of between-group edges. The calculation of the modularity coefficient was determined using the Louvain algorithm (30).

Hubs. In this study, network hubs are defined as the most efficient nodes in a network, i.e. those with the highest E_{nodal}. For each node i, if the normalised (divided by the mean E_{nodal} of all nodes) $E_{nodal}(i)$ is larger than the normalised mean E_{nodal} of all nodes in a network plus one standard deviation (SD), the node is considered a hub region (31).

In addition to the hub classification based on E_{nodal}, a set of hubs were classified by analysis of the distribution of connections within and between modules, allowing the categorization of hub regions into provincial and connector hubs, as described below.

Provincial hubs were defined as the nodes with a high within-module degree centrality (within module z-score greater than the mean plus SD of all nodes), indicating its central role in intra-modular communication, and low participation coefficient (PC) (PC≤0.3). Participation coefficient or proportion of cross-module connectivity profile compares the number of links of a given node to other nodes in different communities, to the total number of links to other nodes in the same community. This measure is defined as:

$$PC(i) = 1 - \sum_{c=1}^{N_C} \left(\frac{k_{C_i}}{k_i} \right)^2 ,$$

Connector hubs were defined as regions with a high value of within-module degree centrality and participation coefficient (PC>0.3), indicating a high proportion of cross-module connectivity, and thus a central role in the inter-modular communication. Upon identifying connector-hubs, we further characterized their connectivity to the rest of the network.

Rich club

By definition, a set of brain areas in the network shows a rich club structure if its level of interconnectivity exceeds the level of connectivity expected on basis of chance alone (29). In particular, the weighted rich club coefficient $\Phi(k)$ is computed as the ratio between the weights of connections present within the subnetwork *S*, composed of regions with a degree > k, and the total sum of weights present within an equally sized subset of the top ranking connection-weights in the network. The normalized rich club coefficient $\Phi_{norm}(k)$ is computed by dividing $\Phi(k)$ by $\Phi_{random}(k)$, with $\Phi_{random}(k)$ calculated as the average rich club coefficient for each *k* of a set of 1000 randomized graphs (preserving the degree distribution) (29). Therefore, a structural brain network can be described as having a rich club organization if, for a given degree interval, the normalized rich club coefficient is greater than 1.

The integrative nature of rich club members by the linking of different communities was also assessed. For this, we identified "rich-connector-hub networks". These were constructed by examining the

connectivity profile of nodes that simultaneously qualified as rich-club members and connector hubs (as defined above), to the remaining connector hubs in the network .

Between-group differences in structural connectivity strength

Between-group statistical comparison of the raw structural connectomes for PBD patients and controls was performed on a connection-by-connection basis, using a non-parametric statistical method – network-based statistics (NBS). This method allows the identification of significantly altered sub-networks, while controlling for the family-wise error rate (FWER) (32). The NBS was used with a primary statistical threshold of t=2.1. The topological configuration of a group effect in structural connectivity strength was then represented by one or multiple significantly connected components with FWER-corrected $p<0.05$.

Between-group significant differences in Graph measures

Between-group statistical comparison was performed using M-W U test, KS-test and T-test.

Relationship between network metrics and neurocognitive scores

The neurocognitive scores (coding and FSIQ) assessed for the HC and PBD groups, as well as the positive and negative symptoms scores (PANNS) assessed in the PBD patients, were correlated with local and global network properties. Partial correlation analysis was performed, using age and gender as confounding variables. Similarly, the correlation between clinical scores and the subset of network nodes revealing significant group differences in nodal efficiency were also assessed using age and gender as confounding variables.

Results

Demographics

No significant differences were found for age (p=0.30), gender (p=1), verbal IQ (p=0.20), performance IQ (p=0.16) and FSIQ (p=0.13) scores between patients with Pediatric Bipolar Disorder (PBD) and healthy controls (HC) (Table 1).

Connectivity Strength

Compared to controls, patients with PBD showed significantly altered structural connectivity (p=0.015) in a brain sub-network, or connected component, involving 71 structural links (~1,8% of all possible connections; ~5,5% of all existing connections) (Figure 1). These 71 links showed 39 decreases and 32 increases in connectivity strength in the PBD group (see Supplementary Table 1 for details). The network is predominantly distributed in right frontal inferior and temporal brain areas (22% more connections on the right hemisphere).

Graph Theoretical Analysis: Local Properties

Nodal efficiency - network hubs

For each group, regions showing a high normalized nodal efficiency were identified as network hubs. Between-group differences found in the network hub configuration are suggestive of local asymmetries in efficiency of communication (Figure 2).

In the HC group, 13 hub areas were identified (Figure 2a; Supplementary Table 2). The hub configuration for the PBD group revealed the loss of five hubs and inclusion of one new hub when compared to the HC group. Of particular interest are the exclusivity of the medial orbitofrontal and inferior temporal (bilateral) hubs to healthy controls.

Graph Theoretical Analysis: Global properties

No significant network differences were found between the HC and PBD structural connectomes on any of the global graph measures assessed: global efficiency, modularity, clustering coefficient, characteristic path length and small-worldness (see Supplementary Table 5).

Modularity and Hub Classification

For each group, the whole-brain optimal community structure was decomposed into seven modules as shown in Figures 3A and 3C. The HC and PBD groups revealed differences in their modular arrangement, with the most important changes found in the right lateral and the medial posterior regions of the brain.

Rich club

Rich club organisation was found in the structural networks of both HC and PBD patients. The group-weighted and normalised rich club coefficient curves of both HC and PBD, shows that the maximal $\Phi_{norm}(k)$ is reached at k=35 for both groups. However, as illustrated in Figure 4A, the peak amplitude is clearly decreased in the patient group, which is indicative of a reduced rich club organisation for this group. This reveals lower level of connectivity between the most densely connected regions in the brain, when compared with the HC group. Additionally, rich club membership between groups differed only in two right hemisphere nodes, suggesting that the insular cortices and the hippocampus have a rich club profile exclusive to the PBD group (Figure 4B).

As described in Methods section *Rich Club*, we also examined the connectivity profile of nodes that simultaneously qualified as rich-club members and connector hubs to the other connector hubs in the network (Figure 4C). These networks revealed a relatively symmetric connectivity pattern and central spatial distribution in the HC group, involving regions of the right posterior cingulum and amygdala, left precuneus and left and right hippocampus and putamen (Figure 4C (bottom)). This strong 'core-effect', supported by a structural network of rich-connector-hubs linking functionally different communities, reflects a tendency toward efficient integration of information across the brain, in the HC group. In contrast, the PBD group exhibited a comparatively asymmetric profile of 'rich-connector-hub' connectivity (Figure 4C (top)). This tendency toward spatially unbalanced modular integration was characterised by a deficit of two right hemisphere rich-connector-hubs (loss of the hippocampus, amygdala and putamen; gain of the superior occipital gyrus), when compared to the HC group, resulting in a single right hemisphere module (posterior) being comprised in this network, as opposed to two right-hemisphere modules in the HC group.

Network properties vs. neurocognitive and psychotic symptoms

We examined the relationship of neurocognitive scores – coding, VIQ, PIQ, FSIQ – and psychotic symptoms with both the nodal efficiency of regions showing significant group differences (Supplementary Table 3) and the various global graph properties assessed (Supplementary Table 4).

It is only for the orbitofrontal cortex that nodal efficiency was significantly correlated with IQ and/or psychotic symptoms (PANSS) . Nodal efficiency of the left inferior orbitofrontal cortex was significantly positively correlated with the VIQ (r=0.74; p=0.04), PIQ (r=0.60; p=0.03) and FSIQ (r=0.77; p=0.02) scores, whereas negative psychotic symptoms were positively correlated with the nodal efficiency of the left middle orbitofrontal cortex (r=0.57; p=0.04) (Figure 5).

None of the global network metrics assessed showed significant correlation with the neurocognitive/psychotic scores (Supplementary Table 4).

Discussion

We investigated the topological organisation of the structural connectomes in a cohort of adolescents with a diagnosis of PBD with psychosis Network analysis using a combination of state-of-the-art methods revealed significant differences in structural connectivity between PBD patients and healthy matched participants. Most differences were found in networks involved in emotional regulation, strengthening the hypothesis that BD could be linked to prefrontal top-down dysregulation of emotional processing. Specifically, we found widespread differences in structural connectivity strength, and altered hub configuration and connectivity profile. |Changes were also found in the rich-club organisation of the PBD structural network and in inter-modular connectivity pattern driven by 'rich-connector-hubs'.

These findings suggest that key network features for balanced whole-brain integration of information are altered in PBD. In addition, our results demonstrate that the nodal efficiency of regions important for the regulation of emotional processing such as the orbitofrontal cortex show significant positive correlations with IQ scores and negative symptoms in PBD patients. Overall, these findings of abnormal topological organization in PBD shed new light on the potential neurobiological mechanisms underlying BD.

The widespread alterations in structural connectivity in the PBD brain networks (shown in Figure 1), primarily differ from HC in inferior temporal networks and inferior frontal networks and subcortical to inferior frontal regions (Figure 1; Supplementary Table 1). This fits well with previously reported localised changes in white matter, where there is evidence for a loss of connectivity involving prefrontal and frontal regions through associative and commissural fibres (33,34). Widespread *decreases* in fractional anisotropy (FA) have been found in major tracts, including (but not limited to) the orbitofrontal cortex (18), superior frontal lobes (15,34), and bilateral parietal and occipital corona radiate (17). It has indeed been suggested that white matter changes could be central to BD, and may represent an endophenotype (36). Our findings of widespread connectivity changes in PBD support this idea but add significant information on the specific affected structurally connectivity networks.

Our structural connectivity findings are also consistent with the previously reported widespread changes in regional grey matter volumes in PBD. Specifically, neuroimaging studies have linked PBD (37) to altered cortical grey matter volumes in several regions shown to have abnormal structural connectivity in the present study, including (but not limited to) the basal ganglia (38), thalamus (38)

and temporal cortices (38,39), cingulate (37–40), dorsolateral prefrontal cortex (DLPFC) (41,42), temporal lobe (2,38,43), orbitofrontal cortex (OFC) (38,41,2,42), and the amygdala The substantial overlap between previously reported grey matter changes and the structural connectivity changes demonstrated here, are suggestive of a mechanistic link between the volume of cortical and subcortical regions involved in emotional regulation and their structural connectivity to the rest of the brain.

Furthermore, our structural connectivity findings can be thought of in terms of providing the supporting connectome for the previously observed *functional* connectivity changes in PBD. The structural changes in PBD are likely to lead to changes in functional brain activity, Thus far few studies investigating resting state functional connectivity in BD have been published, but changes in the functional connectivity of the orbitofrontal cortex (2,38,44), amygdala (45) and temporal lobe (38,46) have been reported. One particular study analysed resting state networks in BD during the manic state and showed significant changes in resting state connectivity, mainly involving regions associated with the fronto-temporal, ventral-affective and dorsal-cognitive circuits (47). These observations are consistent with the present structural connectivity findings (e.g. temporal pole to amygdala, amygdala to parahippocampal gyrus, superior frontal gyrus and pallidum, between orbitofrontal cortices, caudate and pallidum to orbitofrontal cortices) and, taken together, strengthen the hypothesis that functional network dysregulation supported by abnormal structural connectivity, is a prominent driver of pathophysiology in PBD.

The results from our graph theoretical analysis of the PBD connectome also revealed significant changes on the nodal efficiency measure with a loss of five hubs (right orbitofrontal cortex, left cuneus, bilateral temporal gyrus and left occipital cortex) in PBD relative to HC. These brain regions have been demonstrated to be involved in emotional processing and regulation (48,49) As such, these changes are consistent with the previously reported abnormal prefrontal top-down dysregulation in BP (4,50).

We further investigated the whole-brain optimal community structure for the PBD and HC. The networks were decomposed into seven modules and we found that the healthy controls and PBD groups showed differences in their modular arrangements, with the most important changes found in the community assignments of lateral and medial inferior posterior brain regions.

The potential functional relevance of these modularity changes can notably be characterised by investigating the rich club organization. Interestingly, at peak amplitude k=35 for the HC, we found the degree of rich club organisation in PBD to be lower than in HC. This considerable reduction in rich

club organisation reveals lower connectivity between topologically central hub regions of the brain, compared with the healthy participants. To further characterize these changes, we analyzed the networks of structural inter-modular connectivity that are driven by 'rich-connector-hubs'; that is rich-club members that also qualified as connector hubs with high betweenness-centrality and high participation coefficient. Despite the considerable level of overlap in the rich club membership between groups, the integrative nature (participation in inter-modular connectivity) of rich-club members revealed a clear difference in the spatial distribution and number of involved modules, which is suggestive of a disruptive neural network integration capability in the PBD group. Specifically, a single right hemisphere module (posterior) was comprised in the rich-connector-hub network, which may reflect a tendency toward weaker global network integration in the PBD group.

We also demonstrated that the nodal efficiency of two subdivisions of the orbitofrontal cortex, is significantly correlated with IQ scores and negative symptoms in PBD patients, consistent with prior studies involving the orbitofrontal cortex in emotional processing (48). Furthermore, structural connectivity changes may result not only in the emotional dysfunction seen in PBD but also in significant cognitive deficits as revealed in a recent meta-analysis of verbal learning and memory, processing speed, and executive dysfunction (51).

In summary, our results show that there are significant changes in structural connectivity between patients with early–onset bipolar disorder with psychosis compared to healthy matched participants. These changes are primarily manifested in reduced connectivity between inferior, frontal and temporal cortical areas and to regions linked to emotion, memory and executive function, such as amygdala, hippocampus and the basal ganglia. Taken together, these findings suggest that PBD is characterised by a dysfunctional prefrontal regulatory mechanism in line with the hypothesis of prefrontal top-down dysregulation in BD (4,50). Furthermore, differences in the structural network's topological organisation suggest a significant reduction of overall integrative processing capability, that is associated with the patients' neurocognitive faculties and symptoms. These changes may potentially explain the deficits in emotion processing and regulation found in PBD, and ultimately lead to the development of more targeted treatments.

References

1. Mahon K, Burdick KE, Szeszko PR. A Role for White Matter Abnormalities in the Pathophysiology of Bipolar Disorder. Neurosci Biobehav Rev. 2010 Mar;34(4):533–54.

2. James A, Hough M, James S, Burge L, Winmill L, Nijhawan S, et al. Structural brain and neuropsychometric changes associated with pediatric bipolar disorder with psychosis: Imaging pediatric bipolar disorder. Bipolar Disord. 2011 Feb;13(1):16–27.

3. Strakowski SM, Eliassen JC, Lamy M, Cerullo MA, Allendorfer JB, Madore M, et al. Functional Magnetic Resonance Imaging Brain Activation in Bipolar Mania: Evidence for Disruption of the Ventrolateral Prefrontal-Amygdala Emotional Pathway. Biol Psychiatry. 2011 Feb 15;69(4):381–8.

4. Phillips ML, Swartz HA. A critical appraisal of neuroimaging studies of bipolar disorder: toward a new conceptualization of underlying neural circuitry and roadmap for future research. Am J Psychiatry. 2014 Aug 1;171(8):829–43.

5. Nusslock R, Almeida JR, Forbes EE, Versace A, Frank E, LaBarbara EJ, et al. Waiting to win: elevated striatal and orbitofrontal cortical activity during reward anticipation in euthymic bipolar disorder adults. Bipolar Disord [Internet]. 2012 May [cited 2016 Oct 3];14(3). Available from: http://www.ncbi.nlm.nih.gov/pmc/articles/PMC3826255/

6. Linke J, King AV, Rietschel M, Strohmaier J, Hennerici M, Gass A, et al. Increased Medial Orbitofrontal and Amygdala Activation: Evidence for a Systems-Level Endophenotype of Bipolar I Disorder. Am J Psychiatry. 2012 Mar 1;169(3):316–25.

7. Wessa M, Houenou J, Paillère-Martinot M-L, Berthoz S, Artiges E, Leboyer M, et al. Fronto-Striatal Overactivation in Euthymic Bipolar Patients During an Emotional Go/NoGo Task. Am J Psychiatry. 2007 Apr 1;164(4):638–46.

8. Pavuluri MN, Passarotti AM, Harral EM, Sweeney JA. An fMRI Study of the Neural Correlates of Incidental Versus Directed Emotion Processing in Pediatric Bipolar Disorder. J Am Acad Child Adolesc Psychiatry. 2009 Mar;48(3):308–19.

9. Altshuler L, Bookheimer S, Townsend J, Proenza MA, Sabb F, Mintz J, et al. Regional brain changes in bipolar I depression: a functional magnetic resonance imaging study. Bipolar Disord. 2008 Sep;10(6):708–17.

10. Foland LC, Altshuler LL, Bookheimer SY, Eisenberger N, Townsend J, Thompson PM. Evidence for deficient modulation of amygdala response by prefrontal cortex in bipolar mania. Psychiatry Res Neuroimaging. 2008 Jan 15;162(1):27–37.

11. Bora E, Fornito A, Yücel M, Pantelis C. Voxelwise Meta-Analysis of Gray Matter Abnormalities in Bipolar Disorder. Biol Psychiatry. 2010 Jun 1;67(11):1097–105.

12. Ellison-Wright I, Bullmore E. Anatomy of bipolar disorder and schizophrenia: A meta-analysis. Schizophr Res. 2010 Mar;117(1):1–12.

13. Selvaraj S, Arnone D, Job D, Stanfield A, Farrow TF, Nugent AC, et al. Grey matter differences in bipolar disorder: a meta-analysis of voxel-based morphometry studies. Bipolar Disord. 2012 Mar 1;14(2):135–45.

14. Abé C, Ekman C-J, Sellgren C, Petrovic P, Ingvar M, Landén M. Cortical thickness, volume and surface area in patients with bipolar disorder types I and II. J Psychiatry Neurosci JPN. 2016 Jul;41(4):240–50.

15. Collin G, van den Heuvel MP, Abramovic L, Vreeker A, de Reus MA, van Haren NEM, et al. Brain network analysis reveals affected connectome structure in bipolar I disorder: The Structural Connectome in Bipolar Disorder. Hum Brain Mapp. 2016 Jan;37(1):122–34.

16. Adler CM, Adams J, DelBello MP, Holland SK, Schmithorst V, Levine A, et al. Evidence of White Matter Pathology in Bipolar Disorder Adolescents Experiencing Their First Episode of Mania: A Diffusion Tensor Imaging Study. Am J Psychiatry. 2006 Feb 1;163(2):322–4.

17. Barnea-Goraly N, Chang KD, Karchemskiy A, Howe ME, Reiss AL. Limbic and Corpus Callosum Aberrations in Adolescents with Bipolar Disorder: A Tract-Based Spatial Statistics Analysis. Biol Psychiatry. 2009 Aug 1;66(3):238–44.

18. Kafantaris V, Kingsley P, Ardekani B, Saito E, Lencz T, Lim K, et al. Lower Orbital Frontal White Matter Integrity in Adolescents With Bipolar I Disorder. J Am Acad Child Adolesc Psychiatry. 2009 Jan;48(1):79–86.

19. Goldstein BI, Birmaher B. Prevalence, clinical presentation and differential diagnosis of pediatric bipolar disorder. Isr J Psychiatry Relat Sci. 2012;49(1):3–14.

20. Lewinsohn PM, Klein DN, Seeley JR. Bipolar disorders in a community sample of older adolescents: prevalence, phenomenology, comorbidity, and course. J Am Acad Child Adolesc Psychiatry. 1995 Apr;34(4):454–63.

21. Bullmore E, Sporns O. Complex brain networks: graph theoretical analysis of structural and functional systems. Nat Rev Neurosci. 2009 Mar;10(3):186–98.

22. Bassett DS, Sporns O. Network neuroscience. Nat Neurosci. 2017 Feb 23;20(3):353–64.

23. Deco G, Kringelbach ML. Great Expectations: Using Whole-Brain Computational Connectomics for Understanding Neuropsychiatric Disorders. Neuron. 2014 Dec;84(5):892–905.

24. Tzourio-Mazoyer N, Landeau B, Papathanassiou D, Crivello F, Etard O, Delcroix N, et al. Automated Anatomical Labeling of Activations in SPM Using a Macroscopic Anatomical Parcellation of the MNI MRI Single-Subject Brain. NeuroImage. 2002 Jan;15(1):273–89.

25. Jenkinson M, Bannister P, Brady M, Smith S. Improved Optimization for the Robust and Accurate Linear Registration and Motion Correction of Brain Images. NeuroImage. 2002 Oct;17(2):825–41.

26. Collins DL, Neelin P, Peters TM, Evans AC. Automatic 3D intersubject registration of MR volumetric data in standardized Talairach space. J Comput Assist Tomogr. 1994 Apr;18(2):192–205.

27. Behrens T e. j., Woolrich M w., Jenkinson M, Johansen-Berg H, Nunes R g., Clare S, et al. Characterization and propagation of uncertainty in diffusion-weighted MR imaging. Magn Reson Med. 2003 Nov 1;50(5):1077–88.

28. Behrens TEJ, Berg HJ, Jbabdi S, Rushworth MFS, Woolrich MW. Probabilistic diffusion tractography with multiple fibre orientations: What can we gain? NeuroImage. 2007 Jan;34(1):144–55.

29. Rubinov M, Sporns O. Complex network measures of brain connectivity: Uses and interpretations. NeuroImage. 2010 Sep;52(3):1059–69.

30. Blondel VD, Guillaume J-L, Lambiotte R, Lefebvre E. Fast unfolding of communities in large networks. J Stat Mech Theory Exp. 2008 Oct 9;2008(10):P10008.

31. Lo C-Y, Wang P-N, Chou K-H, Wang J, He Y, Lin C-P. Diffusion Tensor Tractography Reveals Abnormal Topological Organization in Structural Cortical Networks in Alzheimer's Disease. J Neurosci. 2010 Dec 15;30(50):16876–85.

32. Zalesky A, Fornito A, Bullmore ET. Network-based statistic: Identifying differences in brain networks. NeuroImage. 2010 Dec;53(4):1197–207.

33. Brambilla P, Bellani M, Yeh P-H, Soares JC. Myelination in bipolar patients and the effects of mood stabilizers on brain anatomy. Curr Pharm Des. 2009;15(22):2632–6.

34. Heng S, Song AW, Sim K. White matter abnormalities in bipolar disorder: insights from diffusion tensor imaging studies. J Neural Transm. 2010 Jan 27;117(5):639–54.

35. Frazier JA, Breeze JL, Papadimitriou G, Kennedy DN, Hodge SM, Moore CM, et al. White matter abnormalities in children with and at risk for bipolar disorder. Bipolar Disord. 2007 Dec 1;9(8):799–809.

36. Borgwardt S, Fusar-Poli P. White matter pathology--an endophenotype for bipolar disorder? BMC Psychiatry. 2012 Sep 13;12:138.

37. Lim CS, Baldessarini RJ, Vieta E, Yucel M, Bora E, Sim K. Longitudinal neuroimaging and neuropsychological changes in bipolar disorder patients: Review of the evidence. Neurosci Biobehav Rev. 2013 Mar;37(3):418–35.

38. Wilke M, Kowatch RA, DelBello MP, Mills NP, Holland SK. Voxel-based morphometry in adolescents with bipolar disorder: first results. Psychiatry Res. 2004 May 30;131(1):57–69.

39. Gogtay N, Ordonez A, Herman DH, Hayashi KM, Greenstein D, Vaituzis C, et al. Dynamic mapping of cortical development before and after the onset of pediatric bipolar illness. J Child Psychol Psychiatry. 2007 Sep 1;48(9):852–62.

40. Kaur S, Sassi RB, Axelson D, Nicoletti M, Brambilla P, Monkul ES, et al. Cingulate Cortex Anatomical Abnormalities in Children and Adolescents With Bipolar Disorder. Am J Psychiatry. 2005 Sep 1;162(9):1637–43.

41. Dickstein DP, Milham MP, Nugent AC, Drevets WC, Charney DS, Pine DS, et al. Frontotemporal alterations in pediatric bipolar disorder: results of a voxel-based morphometry study. Arch Gen Psychiatry. 2005 Jul;62(7):734–41.

42. Najt P, Wang F, Spencer L, Johnston JAY, Cox Lippard ET, Pittman BP, et al. Anterior Cortical Development During Adolescence in Bipolar Disorder. Biol Psychiatry. 2016 Feb 15;79(4):303–10.

43. Frazier JA, Chiu S, Breeze JL, Makris N, Lange N, Kennedy DN, et al. Structural Brain Magnetic Resonance Imaging of Limbic and Thalamic Volumes in Pediatric Bipolar Disorder. Am J Psychiatry. 2005 Jul 1;162(7):1256–65.

44. Dickstein DP, Rich BA, Binstock AB, Pradella AG, Towbin KE, Pine DS, et al. Comorbid anxiety in phenotypes of pediatric bipolar disorder. J Child Adolesc Psychopharmacol. 2005 Aug;15(4):534–48.

45. Pfeifer JC, Welge J, Strakowski SM, Adler CM, DelBello MP. Meta-analysis of amygdala volumes in children and adolescents with bipolar disorder. J Am Acad Child Adolesc Psychiatry. 2008 Nov;47(11):1289–98.

46. Frazier JA, Breeze JL, Makris N, Giuliano AS, Herbert MR, Seidman L, et al. Cortical gray matter differences identified by structural magnetic resonance imaging in pediatric bipolar disorder. Bipolar Disord. 2005 Dec;7(6):555–69.

47. Xiao Q, Zhong Y, Lu D, Gao W, Jiao Q, Lu G, et al. Altered Regional Homogeneity in Pediatric Bipolar Disorder during Manic State: A Resting-State fMRI Study. PLoS ONE. 2013 Mar 6;8(3):e57978.

48. Kringelbach ML. The human orbitofrontal cortex: linking reward to hedonic experience. Nat Rev Neurosci. 2005 Sep;6(9):691–702.

49. Berridge KC, Kringelbach ML. Pleasure systems in the brain. Neuron. 2015 May 6;86(3):646–64.

50. Strakowski SM, Adler CM, Almeida J, Altshuler LL, Blumberg HP, Chang KD, et al. The functional neuroanatomy of bipolar disorder: a consensus model. Bipolar Disord [Internet]. 2012 Jun [cited 2016 Oct 3];14(4). Available from: http://www.ncbi.nlm.nih.gov/pmc/articles/PMC3874804/

51. Nieto RG, Castellanos FX. A meta-analysis of neuropsychological functioning in patients with early onset schizophrenia and pediatric bipolar disorder. J Clin Child Adolesc Psychol Off J Soc Clin Child Adolesc Psychol Am Psychol Assoc Div 53. 2011;40(2):266–80.

52. Latora V, Marchiori M. Efficient Behavior of Small-World Networks. Phys Rev Lett. 2001 Oct 17;87(19):198701.

53. Bassett DS, Bullmore E. Small-World Brain Networks. The Neuroscientist. 2006 Dec 1;12(6):512–23.

Figures

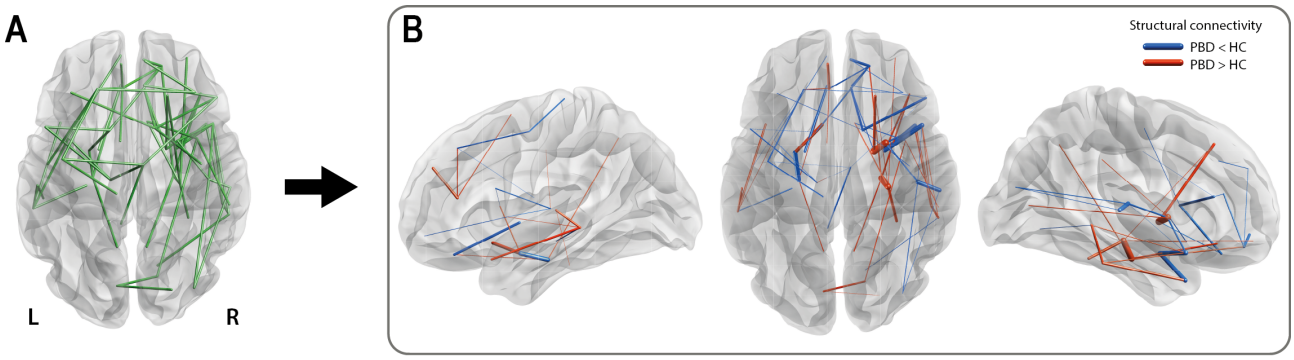

Figure 1. Significant changes in the structural connectivity of patients with pediatric bipolar disorder (PBD) compared with healthy controls (HC). Connected component of significant differences in structural connectivity strength between patients with PBD and HC, represented with edges connecting a pair of regions. **A)** Binarised version of the connected network of significantly altered structural connectivity in PBD. **B)** Weighted version of A), where the edge thickness represents the amplitude of the differences in structural connectivity. Decreases and increases in connectivity strength between regions in the PBD group are represented in blue and red respectively. PBD primarily differs from HC in inferior temporal networks (e.g. left and right temporal pole to left and right amygdala, left amygdala to left parahippocampal region) and inferior frontal networks (e.g. right orbitofrontal cortex) and subcortical to inferior frontal regions (e.g. right caudate to orbitofrontal cortex and left pallidum to left orbitofrontal cortex),

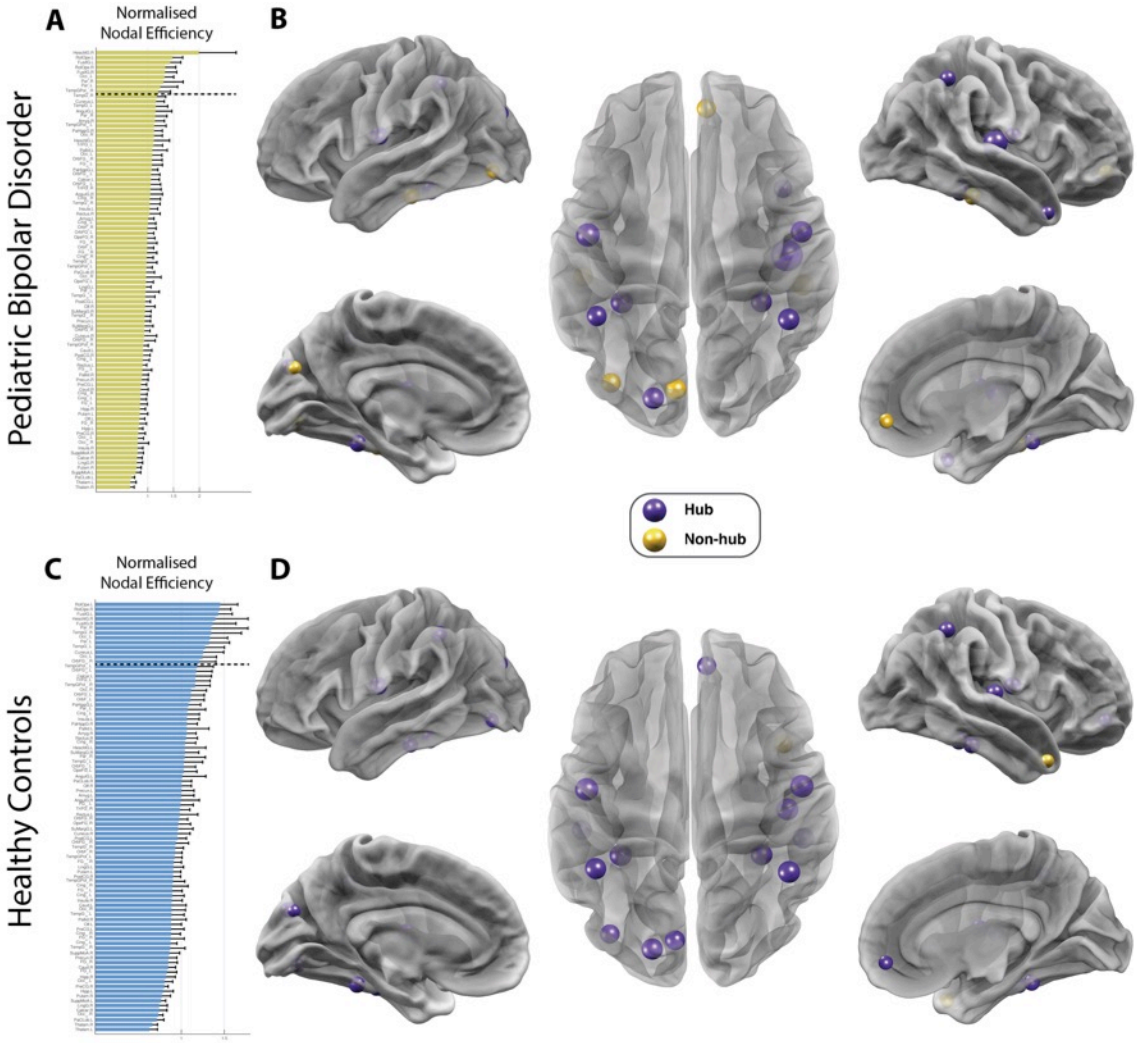

Figure 2. Changes in network hub regions in patients with pediatric bipolar disorder (PBD). Differences in network hub regions in HC (top row) and PBD (bottom row) as measured by the normalised nodal efficiency for all 90 AAL brain regions. This shows a clear reorganisation in hub regions in PBD where e.g. the orbitofrontal cortex is no longer a hub region,. **A)** For the patient group, the figure shows the nodal efficiency sorted according to the mean in descending order. For each node, the E_{nodal} is normalised by the mean of all nodes' E_{nodal}, and a node is identified as a hub region if its normalised E_{nodal} is larger than the sum of the mean plus the SD of all network nodes' E_{nodal}. **B)** Hub regions, represented as spheres positioned according to the centroid stereotaxic coordinates of the correspondent anatomical region, with node size proportional to their E_{nodal}, are mapped onto a 3D reconstructed brain surface. **C)** The ranking of nodal efficiency, and **D)** the identified hub regions for healthy participants. For each group, the existing hub nodes are represented in purple and non-hub nodes (hubs exclusive to the other group) in yellow.

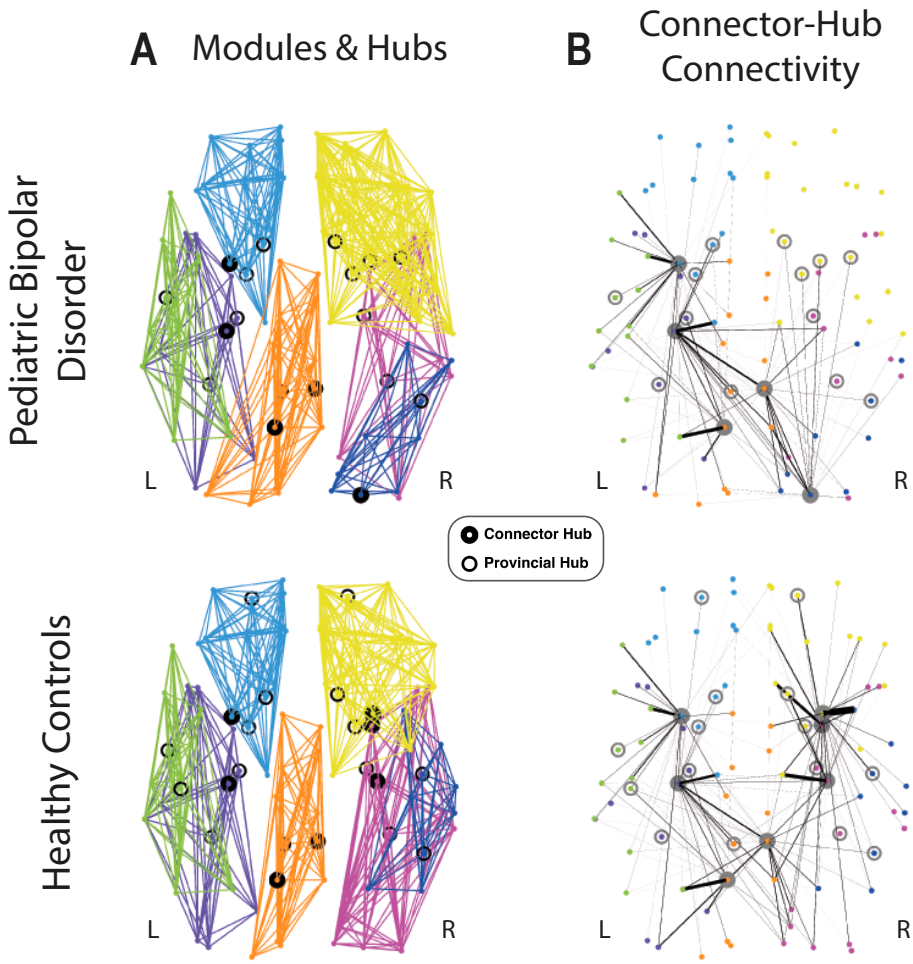

Figure 3. Disrupted modularity, hubs and connector-hub connectivity in patients with pediatric bipolar disorder (PBD). The figure shows the changes in the optimal community structure, i.e. the seven modules and connector hubs shown on a dorsal view of the brain of patients with PBD (top row) and healthy controls (HC, bottom row), with node colours denoting membership to a module and with intra-module edges coloured accordingly. *Connector hubs* (marked as filled circles) are defined as regions with high within-module degree centrality and a participation coefficient $p>0.3$, denoting a high proportion of cross-module connectivity. *Provincial hubs* (marked as unfilled circles) are defined as having high within-module degree centrality but participation coefficient $p\leq0.3$. **A)** Dorsal view of the optimal modularity partitioning found in PBD (top), reveals a different configuration compared to HC (bottom). **B)** Significant local changes are found in the undirected structural connectivity profile for the connector hubs in PBD (top) compared to HC (bottom). Edges, coloured in black, correspond to the structural connectivity of each connector hub region to any other region in the brain, with thickness proportional to its connection strength. Colour of dots represents the belonging of a brain area to a particular community, consistent with A). Albeit the number of both provincial and connector hubs is preserved between the two groups (Supplementary Table 2), variance in the distribution reflects the high impact on the regional dispersion and density of connector-hub-connectivity (CHC), i.e. network of undirected connections involving connector hubs. Whilst there is an almost symmetric distribution of provincial and connector hubs in the HC group, asymmetries found in the hub distribution in the PBD group led to a significantly decreased CHC density in the right anterior hemisphere and a shift of the CHC towards posterior areas of the brain, as shown in **B)**. Notably, the connection between the orbitofrontal provincial hub and the amygdala connector hub is missing in the patient group.

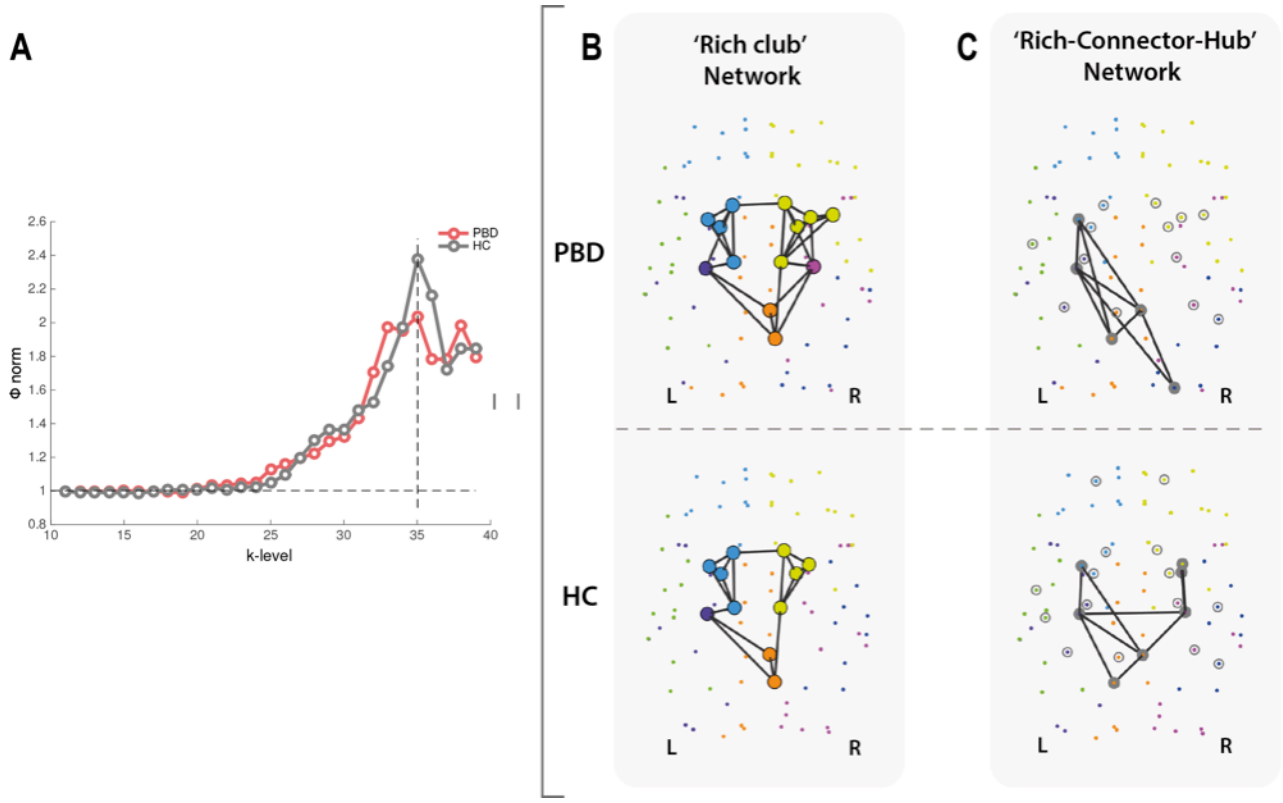

Figure 4. Significant changes in rich club organisation and inter-modular integration in pediatric bipolar disorder (PBD). A) The figure shows significant changes in the rich club organisation as demonstrated by the normalised weighted rich club coefficient as a function of *k*-level (degree), for the PBD (red curve) and healthy control (HC, grey curve) groups. **B)** Rich-club members in HC (bottom) and PBD (top). Rich club nodes are represented by large filled circles with colours denoting the module to which they belong. Rich club member regions common to both groups included the left hippocampus, right posterior cingulate cortex and precuneus, and left and right caudate, putamen, pallidum and thalamus. Membership between groups differed only in two right hemisphere nodes, suggesting that the insular cortices and the hippocampus have a rich club profile exclusive to the PBD group. **C)** Equally, the 'rich-connector-hub' network signature, i.e. the backbone of inter-modular connectivity driven by connector-hubs, is different between the HC (top) and PBD (bottom). Edges coloured in black represent the existing structural connectivity between connector hubs.

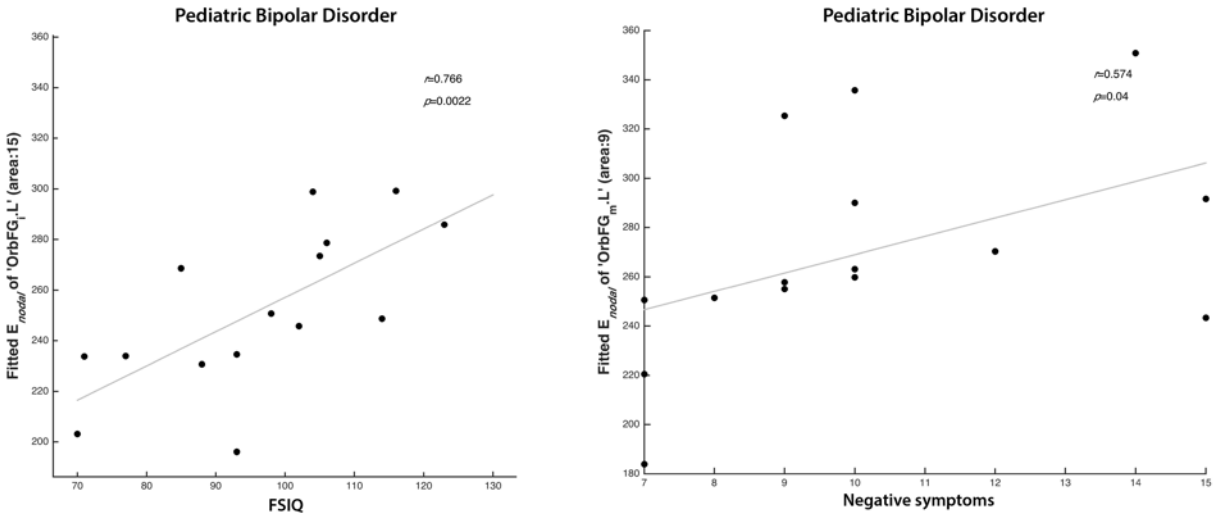

Figure 5. Nodal efficiency of the orbitofrontal cortex in a whole-brain structural connectivity network correlates with psychotic and IQ scores of patients with pediatric bipolar disorder (PBD). Left: A significant positive correlation is found between the nodal efficiency of left inferior orbitofrontal cortex and FSIQ. **Right:** A significant positive correlation is also found between the nodal efficiency of the middle orbitofrontal cortex and negative psychotic symptoms in the PBD group assessed with the PANSS (see Supplementary Table 3 for full details).

Tables

Table 1. Demographic and clinical characteristics of participants

Characteristic	Normal Controls		Patients with PBD		p-value
	mean	SD	mean	SD	
Gender, M/F	8/7	-	8/7	-	1
Handedness, R/L	13/2		13/2		1
Age at onset of symptoms, years	15.70	1.26	15.04	2.04	0.30
Disease duration, years			14.00	2.00	
Verbal IQ	103.60	19.66	94.80	17.03	0.20
Performance IQ	106.53	12.98	99.13	15.01	0.16
Full Scale IQ	105.47	16.37	96.33	16.04	0.13
Coding	-	-	81.33	19.77	-
PANSS: positive scores	-	-	19.27	3.92	-
PANNS: negative scores	-	-	10.13	2.72	-
Beck Depression Inventory			6.60	1.40	
Young Mania Rating Scale			1.40	0.80	
Comorbidity (ADHD), n			5/15		
Medication, n					
Olanzapine			7		
Quetiapine			3		
Risperidone			1		
Fluoxetine			1		
Sodium valproate			2		
Lithium			3		

PANSS = Positive and Negative Syndrome Scale; ADHD = attention-deficit hyperactivity disorder.